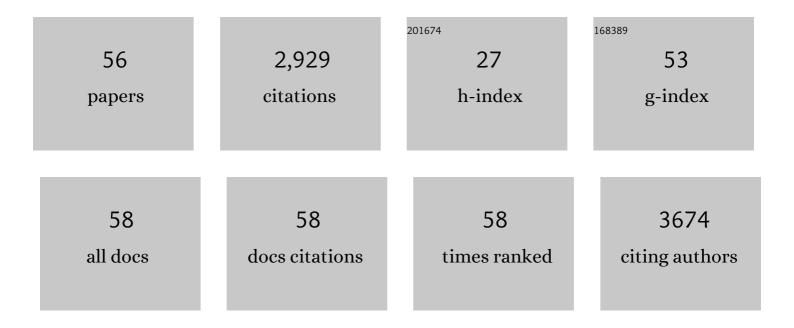
List of Publications by Year in descending order

Source: https://exaly.com/author-pdf/7204716/publications.pdf Version: 2024-02-01



LEI FAN

#	Article	IF	CITATIONS
1	In vivo guiding nitrogen-doped carbon nanozyme for tumor catalytic therapy. Nature Communications, 2018, 9, 1440.	12.8	759
2	Copper/Carbon Hybrid Nanozyme: Tuning Catalytic Activity by the Copper State for Antibacterial Therapy. Nano Letters, 2019, 19, 7645-7654.	9.1	257
3	Carbon-nanoparticles encapsulated in hollow nickel oxides for supercapacitor application. Journal of Materials Chemistry, 2012, 22, 16376.	6.7	154
4	Nitrogen-enriched meso-macroporous carbon fiber network as a binder-free flexible electrode for supercapacitors. Carbon, 2016, 107, 629-637.	10.3	130
5	Tumor Catalytic–Photothermal Therapy with Yolk–Shell Gold@Carbon Nanozymes. ACS Applied Materials & Interfaces, 2018, 10, 4502-4511.	8.0	130
6	Mesoporous Hybrid Shells of Carbonized Polyaniline/Mn ₂ O ₃ as Non-Precious Efficient Oxygen Reduction Reaction Catalyst. ACS Applied Materials & Interfaces, 2016, 8, 6040-6050.	8.0	103
7	Decavanadates anchored into micropores of graphene-like boron nitride: Efficient heterogeneous catalysts for aerobic oxidative desulfurization. Fuel, 2018, 230, 104-112.	6.4	97
8	Growth of Dendritic Silver Crystals in CTAB/SDBS Mixed-Surfactant Solutions. Crystal Growth and Design, 2008, 8, 2150-2156.	3.0	94
9	Mn ²⁺ -coordinated PDA@DOX/PLGA nanoparticles as a smart theranostic agent for synergistic chemo-photothermal tumor therapy. International Journal of Nanomedicine, 2017, Volume 12, 3331-3345.	6.7	78
10	Light-enhanced sponge-like carbon nanozyme used for synergetic antibacterial therapy. Biomaterials Science, 2019, 7, 4131-4141.	5.4	74
11	Template-free synthesis of Ni ₇ S ₆ hollow spheres with mesoporous shells for high performance supercapacitors. CrystEngComm, 2015, 17, 1952-1958.	2.6	69
12	Immobilizing Highly Catalytically Molybdenum Oxide Nanoparticles on Graphene-Analogous BN: Stable Heterogeneous Catalysts with Enhanced Aerobic Oxidative Desulfurization Performance. Industrial & Engineering Chemistry Research, 2019, 58, 863-871.	3.7	60
13	Fabrication of Novel CdIn ₂ S ₄ Hollow Spheres via a Facile Hydrothermal Process. Journal of Physical Chemistry C, 2008, 112, 10700-10706.	3.1	57
14	Controllable Synthesis of Gold Nanorod/Conducting Polymer Core/Shell Hybrids Toward in Vitro and in Vivo near-Infrared Photothermal Therapy. ACS Applied Materials & Interfaces, 2018, 10, 12323-12330.	8.0	53
15	Mechanistic Insight into the Light-Irradiated Carbon Capsules as an Antibacterial Agent. ACS Applied Materials & Interfaces, 2018, 10, 25026-25036.	8.0	51
16	Aloe-Emodin/Carbon Nanoparticle Hybrid Gels with Light-Induced and Long-Term Antibacterial Activity. ACS Biomaterials Science and Engineering, 2018, 4, 4391-4400.	5.2	44
17	Gold Nanorods/Polypyrrole/m-SiO ₂ Core/Shell Hybrids as Drug Nanocarriers for Efficient Chemo-Photothermal Therapy. Langmuir, 2018, 34, 14661-14669.	3.5	43
18	Ultrasmall FeS ₂ Nanoparticlesâ€Decorated Carbon Spheres with Laserâ€Mediated Ferrous Ion Release for Antibacterial Therapy. Small, 2021, 17, e2005473.	10.0	43

#	Article	IF	CITATIONS
19	Mn ₃ O ₄ microspheres as an oxidase mimic for rapid detection of glutathione. RSC Advances, 2019, 9, 16509-16514.	3.6	39
20	One-Pot Synthesis of Fe/N-Doped Hollow Carbon Nanospheres with Multienzyme Mimic Activities against Inflammation. ACS Applied Bio Materials, 2020, 3, 1147-1157.	4.6	39
21	Hybrid shells of MnO2 nanosheets encapsulated by N-doped carbon towards nonprecious oxygen reduction reaction catalysts. Journal of Colloid and Interface Science, 2018, 527, 241-250.	9.4	35
22	High-efficiency platinum–carbon nanozyme for photodynamic and catalytic synergistic tumor therapy. Chemical Engineering Journal, 2020, 399, 125797.	12.7	35
23	Au-PLGA Hybrid Nanoparticles with Catalase-Mimicking and near-Infrared Photothermal Activities for Photoacoustic Imaging-Guided Cancer Therapy. ACS Biomaterials Science and Engineering, 2018, 4, 1083-1091.	5.2	33
24	Pomegranate-like multicore–shell Mn ₃ O ₄ encapsulated mesoporous N-doped carbon nanospheres with an internal void space for high-performance lithium-ion batteries. Chemical Communications, 2019, 55, 8064-8067.	4.1	33
25	Facile and scalable synthesis of nitrogen-doped ordered mesoporous carbon for high performance supercapacitors. Korean Journal of Chemical Engineering, 2020, 37, 166-175.	2.7	31
26	In-situ controllable growth of α-Ni(OH)2 with different morphologies on reduced graphene oxide sheets and capacitive performance for supercapacitors. Colloid and Polymer Science, 2016, 294, 681-689.	2.1	30
27	Au nanoparticle-coated, PLGA-based hybrid capsules for combined ultrasound imaging and HIFU therapy. Journal of Materials Chemistry B, 2015, 3, 4213-4220.	5.8	28
28	Metal ions/nucleotide coordinated nanoparticles comprehensively suppress tumor by synergizing ferroptosis with energy metabolism interference. Journal of Nanobiotechnology, 2022, 20, 199.	9.1	26
29	Pd@aluminium foil: a highly efficient and environment-friendly "tea bag―style catalyst with high TON. Catalysis Science and Technology, 2012, 2, 1136.	4.1	23
30	Using a visible light-triggered pH switch to activate nanozymes for antibacterial treatment. RSC Advances, 2020, 10, 909-913.	3.6	22
31	Multi-Yolk–Shell MnO@Carbon Nanopomegranates with Internal Buffer Space as a Lithium Ion Battery Anode. Langmuir, 2021, 37, 2195-2204.	3.5	22
32	Study on the binding of puerarin to bovine serum albumin by isothermal titration calorimetry and spectroscopic approaches. Journal of Thermal Analysis and Calorimetry, 2010, 102, 217-223.	3.6	21
33	Sn-encapsulated N-doped porous carbon fibers for enhancing lithium-ion battery performance. RSC Advances, 2019, 9, 8753-8758.	3.6	20
34	O/W interface-assisted hydrothermal synthesis of NiCo2S4 hollow spheres for high-performance supercapacitors. Colloid and Polymer Science, 2016, 294, 1325-1332.	2.1	16
35	Improvement in lubricating properties of TritonX-100/n-C 10 H 21 OH/H 2 O lamellar liquid crystals with the amphiphilic ionic liquid 1-alkyl-3-methylimidazolium hexafluorophosphate. Journal of Colloid and Interface Science, 2018, 522, 200-207.	9.4	14
36	Microstructure and Tribological Properties of Lamellar Liquid Crystals Formed by Ionic Liquids as Cosurfactants. Langmuir, 2019, 35, 4037-4045.	3.5	13

#	Article	IF	CITATIONS
37	Reverse intratumor bacteria-induced gemcitabine resistance with carbon nanozymes for enhanced tumor catalytic-chemo therapy. Nano Today, 2022, 43, 101395.	11.9	13
38	Surfactant-mediated preparation and tribological behaviors of few-layer ZnBDC. Materials Letters, 2019, 257, 126757.	2.6	12
39	Photolysis of methicillin-resistant Staphylococcus aureus using Cu-doped carbon spheres. Biomaterials Science, 2020, 8, 6225-6234.	5.4	11
40	Ultrasound-assisted Li+/Na+ co-intercalated exfoliation of graphite into few-layer graphene. Ultrasonics Sonochemistry, 2020, 66, 105108.	8.2	11
41	Artesunate-loaded poly (lactic-co-glycolic acid)/polydopamine-manganese oxides nanoparticles as an oxidase mimic for tumor chemo-catalytic therapy. International Journal of Biological Macromolecules, 2021, 181, 72-81.	7.5	11
42	Lubrication and Dynamically Controlled Drug Release Properties of Tween 85/Tween 80/H ₂ O Lamellar Liquid Crystals. Langmuir, 2021, 37, 7067-7077.	3.5	10
43	Cold nanorod@void@polypyrrole yolk@shell nanostructures: Synchronous regulation of photothermal and drug delivery performance for synergistic cancer therapy. Journal of Colloid and Interface Science, 2022, 610, 89-97.	9.4	10
44	Construction of core-in-shell Au@N-HCNs nanozymes for tumor therapy. Colloids and Surfaces B: Biointerfaces, 2022, 217, 112671.	5.0	10
45	Improved ordering and lubricating properties using graphene in lamellar liquid crystals of Triton X-100/C _n mimNTf ₂ /H ₂ O. Soft Matter, 2020, 16, 2031-2038.	2.7	8
46	Supramolecular Core–Shell Nanoassemblies with Tumor Microenvironmentâ€Triggered Size and Structure Switch for Improved Photothermal Therapy. Small, 2022, 18, e2200588.	10.0	8
47	Heteroatom Bridging Strategy in Carbon-Based Catalysts for Enhanced Oxidative Desulfurization Performance. Inorganic Chemistry, 2022, 61, 633-642.	4.0	8
48	Data of fluorescence, UV–vis absorption and FTIR spectra for the study of interaction between two food colourants and BSA. Data in Brief, 2016, 8, 755-783.	1.0	6
49	N-hydroxyphthalimide anchored on hexagonal boron nitride as a metal-free heterogeneous catalyst for deep oxidative desulfurization. Petroleum Science, 2022, 19, 1382-1389.	4.9	6
50	Interactions of two food colourants with BSA: Analysis by Debye-Hückel theory. Food Chemistry, 2016, 211, 198-205.	8.2	5
51	Doped Nanocarbons Derived from Conducting Polymers toward ORR Electrocatalysts. Advanced Sustainable Systems, 2018, 2, 1800033.	5.3	5
52	Staphylococcus aureus-targeting peptide/surfactant assemblies for antibacterial therapy. Colloids and Surfaces B: Biointerfaces, 2022, 214, 112444.	5.0	5
53	Lubrication performance of MXene/Brij30/H2O composite lamellar liquid crystal system. Colloids and Surfaces A: Physicochemical and Engineering Aspects, 2022, 641, 128487.	4.7	4
54	Brij 30 Induced Transition of Rodlike Micelles to Wormlike Micelles and Gels in the Imidazole Ionic Liquid Surfactants: The Alkyl Chain Length Effect. Langmuir, 2022, 38, 3051-3063.	3.5	4

#	Article	IF	CITATIONS
55	The transition of rodlike micelles to wormlike micelles of an ionic liquid surfactant induced by different additives and the template-directed synthesis of calcium oxalate monohydrate to mimic the formation of urinary stones. Colloid and Polymer Science, 2021, 299, 1991-2002.	2.1	1
56	Fabrication of N-hollow carbon nanospheres@Fe7S8 and their ion-release-based antibacterial properties. Journal of Materials Science, 0, , 1.	3.7	0